



OPEN

## Sugar management and photosynthesis of sugar beet after infection by *Cercospora beticola*

Andrzej Baryga<sup>1</sup>, Szymon Rusinowski<sup>2</sup>, Jacek Krzyżak<sup>2</sup>, Alina Kunicka-Styczyńska<sup>1</sup>, Beata Świącik<sup>1</sup>, Radosław Stec<sup>2</sup>, Krzysztof Smykała<sup>3</sup>, Eugeniusz Małkowski<sup>4</sup> & Krzysztof Sitko<sup>2,4</sup>✉

Sugar beet (*Beta vulgaris* L. subsp. *vulgaris*) is an important crop used not only in sugar production but also as the source of biogas and bioethanol, as a substrate in the petrochemical industry, and as a bio-resource for additional industrial and chemical feedstocks. Sugar beet is sensitive to environmental stress factors, including fungal infections such as *Cercospora beticola* (CLS—Cercospora leaf spot disease). Despite the introduction of plant cultivars with increased resistance to this disease, it causes a significant reduction in crop yield every year. The effect of infection is significant leaf loss in July and August, and the leaf rosette regeneration in September lasts until November. We examined three varieties of sugar beet with increased resistance to CLS. Using satellite images, we monitored the rate of leaf regeneration after CLS infection and studied in detail the gas exchange of plants, the efficiency of the photosynthetic apparatus, changes in the content of pigments and sugars in leaves, and sugar storage in roots. We showed for the first time that leaf regeneration after CLS infection seems independent of sugar accumulated in the roots. Sugar beetroot varieties were characterized by different strategies for managing sugar production and relocation. Moreover, the efficiency of CO<sub>2</sub> assimilation and solar energy absorption were not correlated in time and space in sugar beet, which, in the context of autumn leaf regeneration and senescence, may also be an indication for earlier harvesting.

**Keywords** Cercospora leaf spot, Chlorophyll fluorescence, Sugar polarisation, Sugar storage, Green LAI

Sugar beet (*Beta vulgaris* L. subsp. *vulgaris*) belongs to the *Amaranthaceae* and is a common industrial crop grown commercially in many temperate parts of the world for its high sucrose content. Sugar beet is a biennial crop; however, commercial sugar beet growers regard the crop as an 'annual' harvest before its second year of growth<sup>1</sup>. White sugar, obtained in Europe mainly from the cultivation of sugar beet, is widely used in food processing, distilling, cosmetics, and pharmaceutical industries. Its production in the European Union in the 2023/2024 season, from an area of about 1.5 million hectares, has been estimated at 15.6 million tons. One-fifth of global sugar production also originates from sugar beet<sup>2,3</sup>. The waste generated in sugar production (pulp, petioles, root fragments, and leaves) is used as feed, a source of biomass for biogas plants, or plant fertilizer. Beet leaves with root heads are usually left on plantations and plowed<sup>4–6</sup>, which allows for a reduction in the doses of mineral fertilizers for subsequent cultivation. Beetroot leaves are mainly built of cellulose (13–18%), hemicellulose (11–17%), pectin (14–18%), the main component of which is polygalacturonic acid (PGA), and a small amount of lignin (5–6%). The dry matter of beet leaves is mainly carbohydrates (glucan—11.0%, hemicelluloses—derivatives of xylan, galactan, and arabinan—10.4%, PGA—11.0%), proteins (26.9%), and soluble sugars (10.0%). The seasonal production and distribution of dry matter in sugar beets is relatively constant; initially, more of it is found in the plant shoots, and at the end of the season, it moves as sugar to the root<sup>7</sup>. Most of the changes due to seasonality and location in the dry matter production of the crop are related to the differentiated energy accumulation. The main factors reducing dry matter yield are drought and disease<sup>8,9</sup>. The content of soluble carbohydrates in the leaves and petioles is highest during the ripening beets period and is strongly affected by nitrogen fertilization and weather changes. The protein content of mature leaves was found to be similar in young and mature leaves and is 22 ± 1, 16 ± 1, and 10 ± 3% in dry biomass<sup>10</sup>.

<sup>1</sup>Department of Sugar Industry and Food Safety Management, Faculty of Biotechnology and Food Sciences, Lodz University of Technology, Lodz, Poland. <sup>2</sup>Institute for Ecology of Industrial Areas, Katowice, Poland. <sup>3</sup>QZ Solutions LLC, Opole, Poland. <sup>4</sup>Plant Ecophysiology Team, University of Silesia in Katowice, Katowice, Poland. ✉email: krzysztof.sitko@us.edu.pl

The amount of individual substances accumulated in the leaves is up to 6 times higher than in beetroots. It is assumed that from 1 ton of leaves left in the field, about 3 kg of nitrogen (N), 1 kg of phosphorus ( $P_2O_5$ ), 6.3 kg of potassium ( $K_2O$ ), 0.8 kg of magnesium ( $MgO$ ), 1 kg of calcium ( $CaO$ ), 2.3 kg of sodium ( $Na_2O$ ) and many valuable microelements, such as boron, copper, manganese and zinc, get into the soil. These components are successively made available to plants in the next two or three vegetation seasons. It is assumed that in the first year after plowing in beet leaves, nitrogen is used in 40%, phosphorus—25%, potassium—60%, and magnesium—40%. The leaves should be thoroughly crushed and spread over the field surface, mixed, and plowed to avoid fermentation and acidification of the soil<sup>4</sup>. The size and length of sugar beet foliage varies depending on the season and location and is strongly determined by soil moisture and fertilization. The uptake of large amounts of nitrogen stimulates leaf growth to very large sizes and their formation in the later vegetation period<sup>11</sup>. At the moment of maximum leaf development, the weight of foliage is about 300–400 g d.m.  $m^{-2}$ <sup>12</sup>. The weight of the beetroot heads with leaves is about 50–60 tons per ha (5–6 t/kg of dry matter), depending on the variety, vegetation conditions, and region of cultivation. The chlorophyll content in mature beet leaves is 6.3 mg  $g^{-1}$ , and the differences between the beet varieties are small. The quantitative composition of macro and micronutrients in leaf blades varies depending on age. The concentration of N, P, K, Zn, and Cu decreases with leaf ripening, while the content of Ca, Mg, Na, Mn, and Mo increases.

*Cercospora* leaf spot (CLS) is one of the severe sugar beet diseases caused by *Cercospora beticola*. The occurrence of the disease with high frequency is recorded in the EU, the USA, and Australia, and its distribution is estimated at 30% of the sugar beet cultivation area<sup>13</sup>. A wide development of the disease on the plantation results in a decrease in the accumulation of sucrose in the root, even exceeding 30%, substantially deteriorating the raw material for sugar production, the impoverishment of the fertilizer value of the leaves, and the danger of massive soil contamination with the pathogen<sup>3</sup>. Infected leaves wintering in the soil with conidial spores allow the phytopathogen to survive until the next growing season and penetrate into the parenchyma of leaves mainly through stomata. The first symptoms of CLS appear on the outer leaves of the beet whorls, which are visualized by brownish-grey, round spots with a diameter of 0.5–6 mm (usually from 2 to 5 mm) surrounded by a red, brownish-red, sometimes brown border. In the course of disease development, younger and younger leaves are infected, and visible spots merge and cause fragments of the blade to dry out. The necrosis that forms over time covers the entire surface of the leaf and can also occur on the petioles<sup>14</sup>. The resulting changes in the host tissue are caused by a photoactive toxin, cercosporin, produced by the pathogen<sup>15</sup>. Moreover, other virulence factors: non-host-specific phytotoxin beticolin<sup>16</sup> and effector protein CbNip1 triggering cell necrosis in darkness<sup>17</sup> are fortifying the necrotic effect of cercosporin. Currently, there are no beet varieties that are completely resistant to CLS. There is also no completely effective form of preventing and treating the disease. Therefore, in the area where CLS occurs, the strategy to combat the disease is mainly to minimize economic losses, by trying to develop varieties with increased resistance and conducting spraying during the growing season.

The final effect of CLS in the form of a decrease in the quantity and quality of crops is known, but the mechanisms of the physiological response of plants to this pathogen are not fully understood. Understanding these mechanisms may contribute to a more effective fight against CLS. It is obvious that sugar in beetroots is produced in the leaves during photosynthesis, and CLS attacks and destroys the leaves. The efficiency of the photosynthetic apparatus can be assessed by measuring the efficiency of the dark phase ( $CO_2$  assimilation) and light phase (chlorophyll fluorescence) of photosynthesis<sup>18</sup>. The most important plant pigment for photosynthesis, chlorophyll, is also a recognized sensitive marker of environmental stress<sup>19</sup>. Other pigments present in leaves, flavonols and anthocyanins, function, respectively, as nonenzymatic inhibitors of oxidative stress and protection of the photosynthetic apparatus from excessive UV radiation<sup>20</sup>. All these parameters have a direct impact on the efficiency of photosynthesis and, therefore, may indirectly affect the sugar content in beetroots.

On the one hand, CLS infection may cause a significant decrease in sugar beet yield<sup>21</sup>. On the other hand, the regeneration of leaves by sugar beet may additionally burden the sugar reserves stored in the root, which, however, has not been studied in detail so far. The relationship between photosynthetic efficiency and sugar content in beetroots has not been investigated, especially in the context of CLS infection. It can be hypothesized that the photosynthetic capacity of beetroot will decrease as the growing season progresses, despite the regrowth of leaves. The second hypothesis assumes that leaf regeneration will take place at the expense of reserve material accumulated in the root. Although producers of new varieties guarantee higher resistance to pathogens, we assume in the third hypothesis that the tested varieties will differ in their physiological response to CLS.

The aim of the research was to verify the above hypotheses and check how selected aspects of sugar beet physiology change in the last phase of growth in the context of a previous infection with *Cercospora beticola*. For this purpose, we examined in detail the light and dark phases of photosynthesis and compared the results with changes in the sugar content in sugar beet leaves and roots. This research concept is new to science and may be a starting point for improvement of the methodology of harvesting the sugar beet crop, including its date, based on the physiology of the sugar beet in the context of the *Cercospora beticola* infection.

## Results

### Changes in the green surface area of beet leaves and CLS-infected area during the measurement period

Field satellite image analysis enabled a comparison of the real area of green leaves (Green LAI) of sugar beets between the studied cultivars in selected months (Fig. 1). Plants undergoing CLS infection still retain an abundant crown of dead leaves, which falsifies the LAI reading during *in situ* measurements. Satellite image analysis in September showed that the Jaromir cultivar had the smallest area of live leaves among the studied cultivars (Fig. 1). In October, an increase in the live leaves area of about 30% was measured for all the studied cultivars compared to September. In November, a decrease in the Green LAI value was observed due to autumn senescence (Fig. 1). CLS infection rate (Fig. S1) showed a high negative correlation with Green LAI (correlation

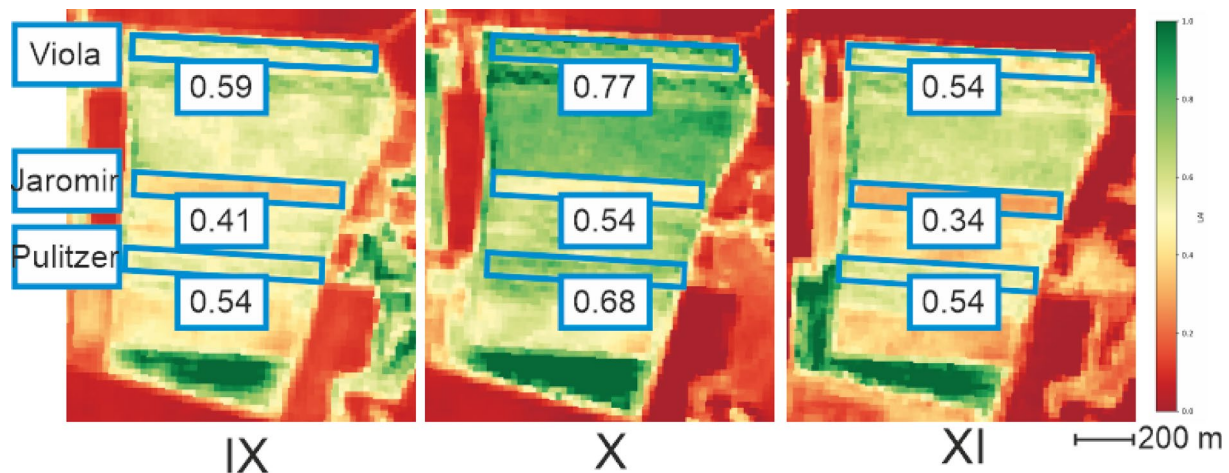


**Fig. 1.** Satellite images with Green LAI imaging of a cultivated field with marked areas occupied by the studied sugar beet varieties in the months of September (IX), October (X) and November (XI). Green LAI values were standardized. The values assigned to each plot in a given month are the Green LAI mean values of the pixel located in the studied area. Obtained satellite images contain modified Copernicus Sentinel data [2024] processed by Sentinel Hub. Data retrieval was done using the LAI (Leaf Area Index) custom script provided by the sentinel hub (<https://custom-scripts.sentinel-hub.com/custom-scripts/sentinel-2/lai/>). Data transformation for visualizations was performed using open-source Python packages (rasterio[1.3.1], geopandas[0.14.4], numpy[1.26.5], pandas[2.2.0], matplotlib[3.8.3]) on the areas of interests.

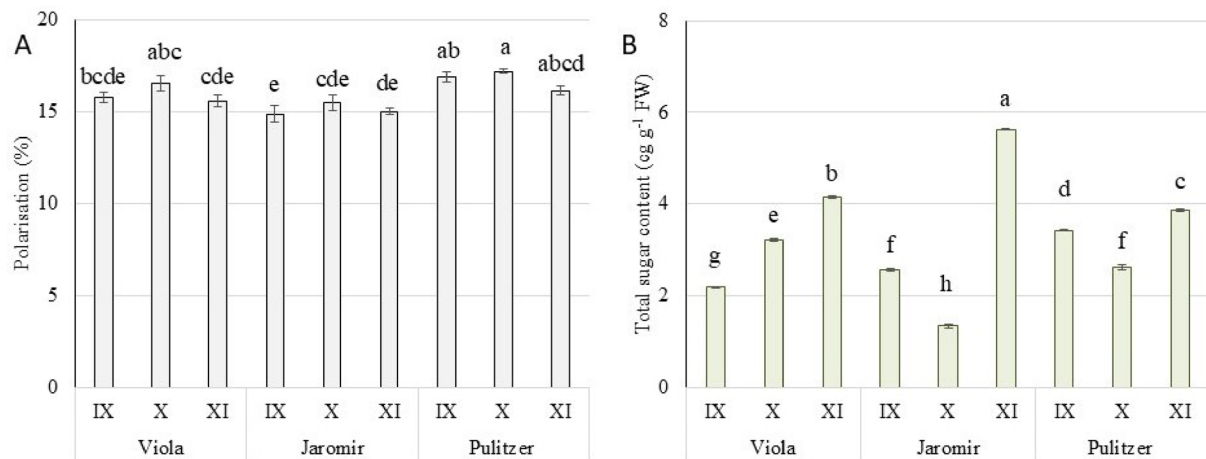


**Fig. 2.** Sugar content in roots (A) and leaves (B) in three sugar beet cultivars (Viola, Jaromir, and Pulitzer) from September (IX) to November (XI). Presented values are means  $\pm$  SE ( $n = 3$ ). Lowercase letters describe statistical significance (ANOVA, LSD test).

$= 0.9$ ) (Fig. S2). The leaves of the Viola cultivar were characterized by the lowest level of CLS infection in October among the tested cultivars (Fig. S1). In November, the number of necroses on the leaves of all the tested cultivars increased compared to October (Fig. S1). This was related to both the action of the pathogen and autumn leaf senescence.

#### Storage material in beetroot roots and leaves

Changes in the total sugar content in beetroot roots and leaves in the examined months of the growing season were illustrated in Fig. 2. Changes in the sugar content in the roots of the tested beets during the last three months of the growing season were not statistically significant within cultivar (Fig. 2A). Nevertheless, their dynamics were similar for all cultivars and indicated the highest sugar content in October (Fig. 2A). The highest total sugar content was recorded in beet leaves in November for all cultivars, and the dynamics of changes depended on the cultivar (Fig. 2B).

The sucrose content in Viola leaves increased significantly with the age of the leaves (Table 1). Glucose, fructose, and fiber reached the highest values in Viola leaves in October and then decreased significantly in

Month	Viola			Jaromir			Pulitzer		
	IX	X	XI	IX	X	XI	IX	X	XI
Sucrose (cg g <sup>-1</sup> )	0.40 ± 0.01 g	1.07 ± 0.03 d	2.23 ± 0.02b	0.48 ± 0.02f	0.18 ± 0.00 h	3.10 ± 0.01a	0.50 ± 0.02f	0.58 ± 0.02e	1.65 ± 0.02c
Glucose (cg g <sup>-1</sup> )	1.31 ± 0.01 d	1.45 ± 0.02b	1.32 ± 0.02 cd	1.40 ± 0.02bc	0.76 ± 0.04f	1.45 ± 0.00b	2.17 ± 0.02a	1.28 ± 0.03 d	1.06 ± 0.03e
Fructose (cg g <sup>-1</sup> )	0.49 ± 0.00f	0.70 ± 0.00 d	0.60 ± 0.01e	0.67 ± 0.01 d	0.41 ± 0.01 g	1.07 ± 0.01e	0.62 ± 0.01e	0.75 ± 0.00c	1.15 ± 0.00a
Fat (cg g <sup>-1</sup> )	0.39 ± 0.01b	0.20 ± 0.00 cd	0.40 ± 0.01b	0.21 ± 0.01c	0.54 ± 0.01c	0.21 ± 0.01c	0.18 ± 0.00 d	0.40 ± 0.00b	4.42 ± 0.00b
Fiber (%)	43.6 ± 0.1 g	45.0 ± 0.1e	43.4 ± 0.0 h	45.5 ± 0.1 d	44.4 ± 0.1f	40.7 ± 0.1i	47.0 ± 0.1a	46.1 ± 0.1c	46.3 ± 0.0b

**Table 1.** Sugar, fat, and fiber content in leaves of Viola, Jaromir, and Pulitzer sugar beet cultivars in different months. Presented values are means ± SE ( $n = 3$ ). Lowercase letters describe statistical significance (ANOVA, LSD test). IX—September, X—October, and XI—November.

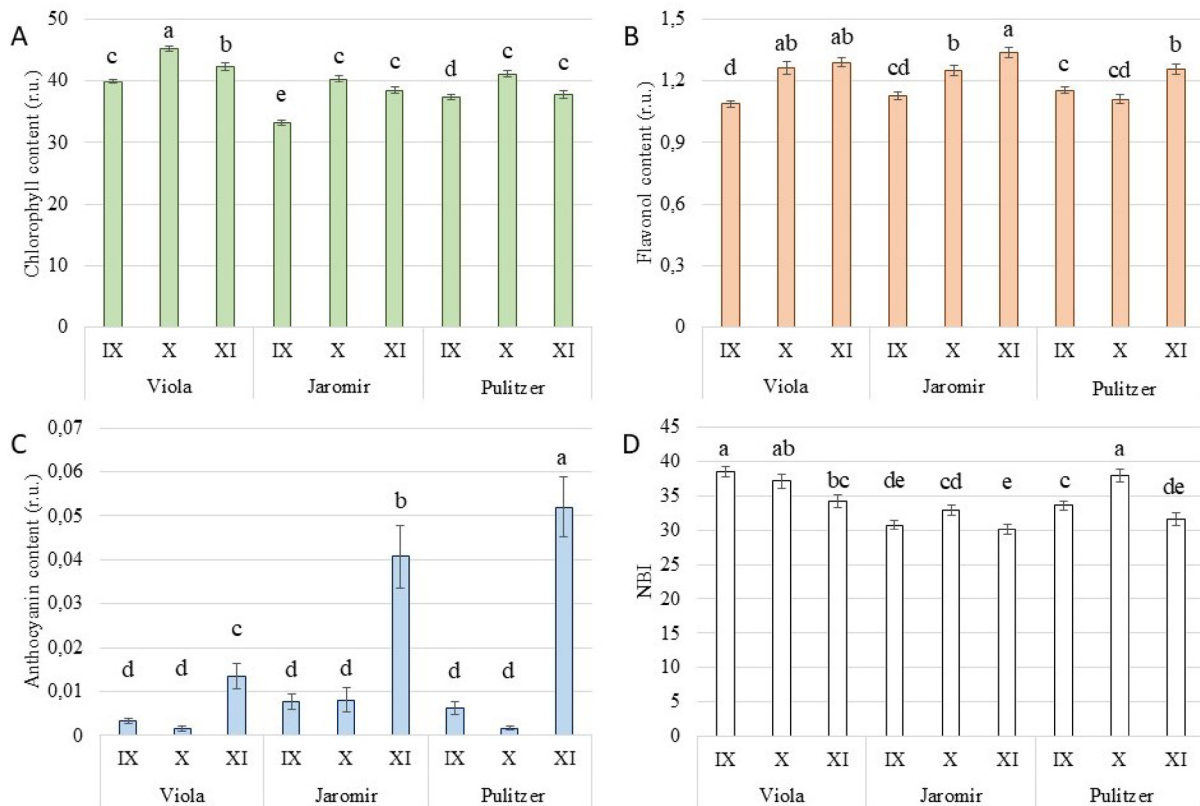


**Fig. 3.** Chlorophyll (A), flavonol (B), and anthocyanin (C) content and Nitrogen Balance Index (D) in Viola, Jaromir, and Pulitzer cultivars of sugar beet from September (IX) to November (XI). Presented values are means ± SE ( $n = 60$ ). Lowercase letters describe statistical significance (ANOVA, LSD test).

November. An inverse relationship occurred in the fat content in Viola leaves, which was the lowest in October (Table 1).

Changes in sucrose, glucose, and fructose content in Jaromir leaves took the form of a U-shaped curve, with a minimum in October (Table 1). The highest fat content in leaves was recorded in October. The fiber content in Jaromir leaves decreased with their age (Table 1).

Sucrose, fructose, and fat content increased in Pulitzer leaves as they aged (Table 1). At the same time, their glucose and fiber content decreased (Table 1).

#### Changes in the content of pigments in beetroot leaves

The highest chlorophyll content in leaves in each month examined was found in the Viola variety, compared to the other beet varieties (Fig. 3A). As the leaves aged, their flavonol content increased in all examined cultivars and changes in these pigments were at a similar level (Fig. 3B). A significant increase in the content of anthocyanins in the leaves of all cultivars took place in November (Fig. 3C). The highest content was recorded in Pulitzer leaves, intermediate in Jaromir, and the lowest content was observed in Viola (Fig. 3C). Nitrogen Balance Index is the ratio of chlorophyll to flavonols in leaves (Fig. 3D). It refers directly to the relationship between primary and secondary metabolism in plants. Viola was characterized by high values of the index in both September and

October, and a significant decrease in the value was noted in November. Jaromir and Pulitzer had the highest NBI values in October and the lowest in November (Fig. 3D).

### Chlorophyll fluorescence as a marker of the state of the photosynthetic apparatus

For the analysis of the relative variable fluorescence ( $\Delta V_t$ ) for all cultivars, the October curve was regarded as a control, and its value for each cultivar is equal to 0 (Fig. 4A). The course of the curves was characteristic for a particular month. For September (IX), a negative ridge was visible with a maximum of around 0.03 s, which could indicate a better performance of the final electron acceptors in PSI (Fig. 4A). This was confirmed by a significant decrease in quantum yield for the reduction of terminal electron acceptors on the acceptor side of PSI ( $\varphi R_0$ ) for Jaromir and Pulitzer (Fig. 4B). The course of the November (XI) curves for Jaromir and Pulitzer was characterized by high peaks with maximums around 0.001 and 0.08 s, which could indicate damage at the  $Q_A^-$  and PSI levels, respectively (Fig. 4A). This course of the curves was reflected in the decrease in the values of the  $\varphi E_0$  and  $\varphi R_0$  parameters (Fig. 4B).

Models of energy fluxes through PSII of excited beet leaf cross-sections clearly showed that the highest PSII efficiency was measured in October (Fig. 5). Leaves of all tested varieties, in September, in the final phase of the *C. beticola* infection, were characterized by the significantly lowest parameters of the percentage of active reaction centers (RC/CS) (Fig. 5). For Jaromir and Pulitzer cultivars, the measurement of absorbed (ABS/CS) and trapped (TR/CS) energy in November returned to the level from September. Moreover, these cultivars were characterized by significantly lower ET/CS and higher RC/CS in November compared to September (Fig. 5). In the case of the Viola cultivar, changes related to senescence were not as pronounced as in the other cultivars. Viola's PSII in November showed a significant decrease in the value of energy flows compared to October, excluding RC/CS (Fig. 5). Nevertheless, November energy flux values were significantly higher than those measured in September (Fig. 5).

### Changes in gas exchange parameters in sugar beets as an effect of CLS and autumn senescence

All tested beet varieties were characterized by the highest transpiration and  $CO_2$  assimilation in September; however, there were significant differences in the values of these parameters between individual cultivars (Fig. 6A, C). In the Viola cultivar, no significant decrease in  $CO_2$  assimilation was observed in November, compared to October, opposite to the photosynthesis rate decrease for the other two varieties (Fig. 6A). The lowest values

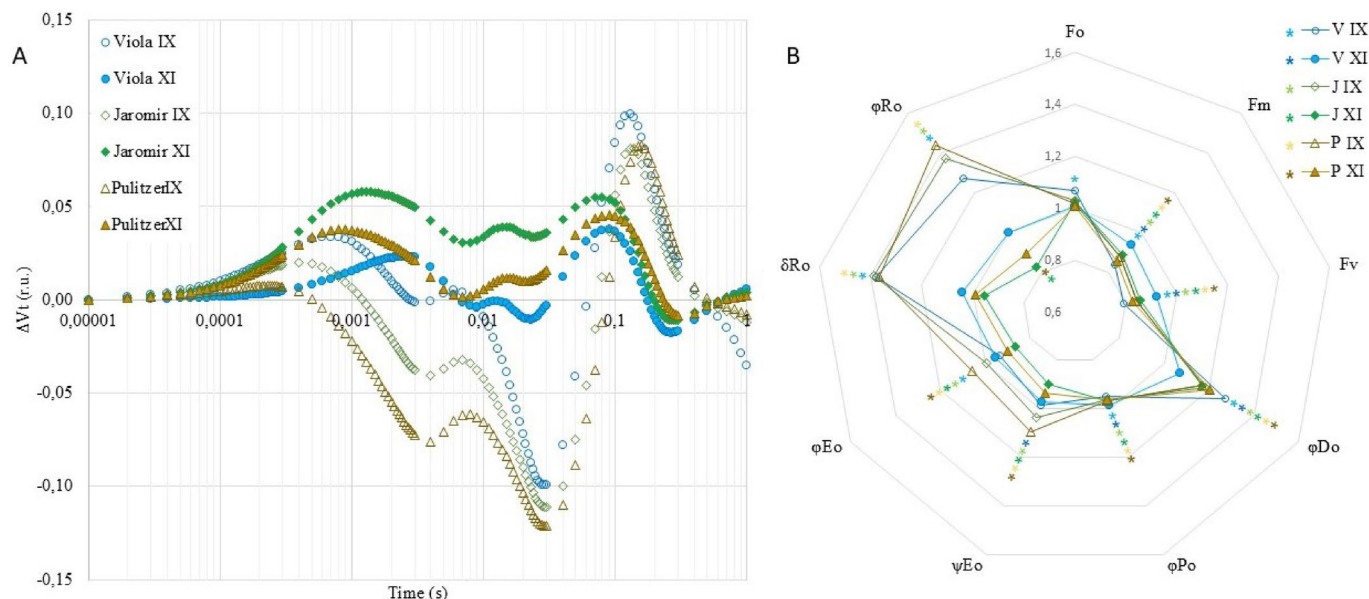


**Fig. 4.** Changes in relative variable fluorescence (A) and fluorescence parameters (B) of the leaves of three sugar beet cultivars: Viola (V), Jaromir (J), and Pulitzer (S), in different months (September—IX, October—X, November—XI). Each relative value of the measured parameters is the mean ( $n = 60$ ). Asterisks plotted on spider chart denote significant differences between reference (October—X, equals 1 for all cultivars) and other months, according to the Fisher LSD test ( $P \leq 0.05$ ). In the Fig. 4A the October curve was also regarded as a control, and its value for each cultivar is equal to 0. Abbreviations:  $F_o$ —minimal fluorescence;  $F_m$ —maximal fluorescence;  $F_v$ —variable fluorescence;  $\varphi P_0$ —maximum quantum yield of primary photochemical reactions,  $\varphi E_0$ —probability (at time 0) that a trapped exciton moves an electron into the electron transport chain beyond  $Q_A^-$ ;  $\varphi E_0$ —quantum efficiency of electron transfer from  $Q_A^-$  to electron transport chain beyond  $Q_A^-$ ,  $\delta R_0$ —probability with which an electron from the intersystem electron carriers will move to reduce the end acceptors at the PSI acceptor side;  $\varphi R_0$ —quantum yield for the reduction of terminal electron acceptors on the acceptor side of PSI.

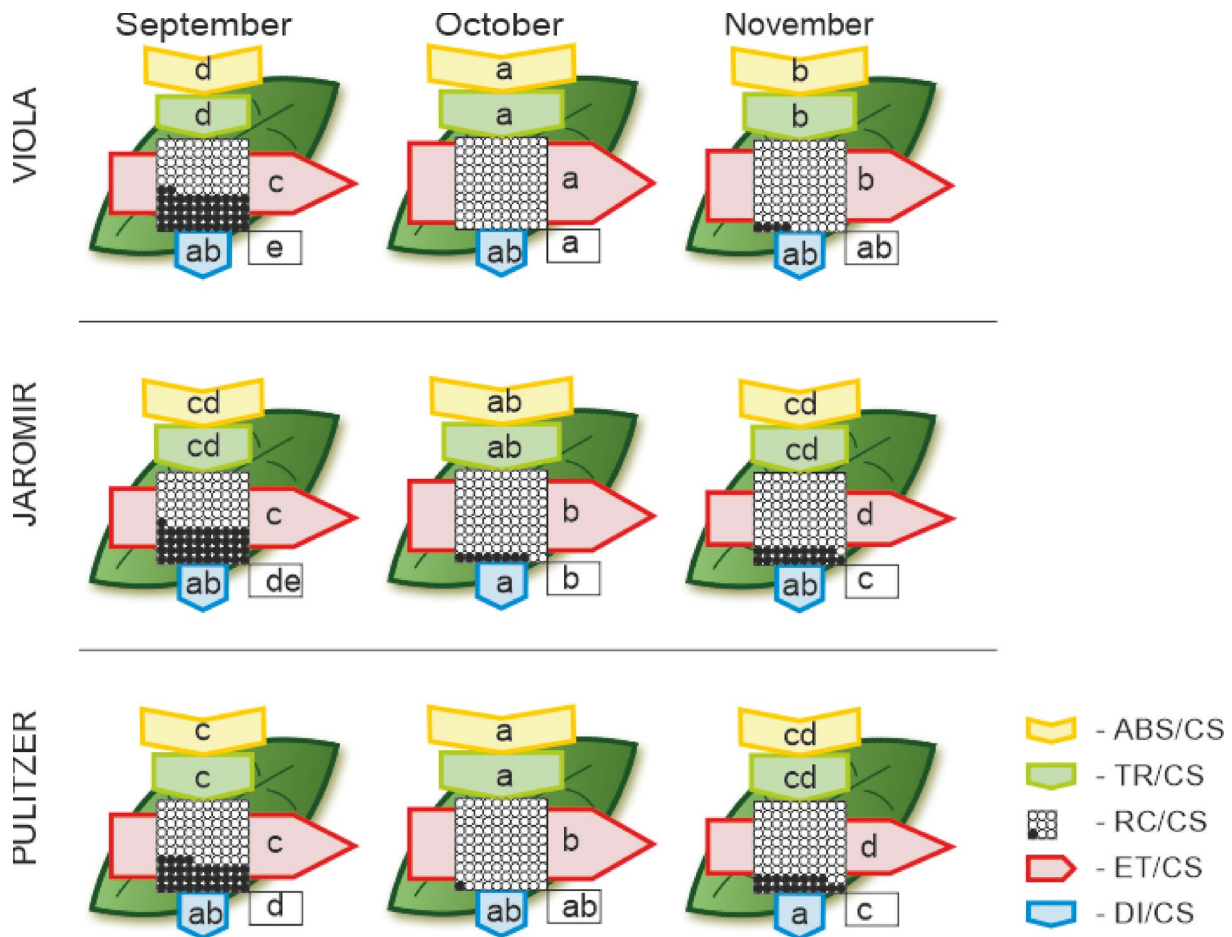


**Fig. 5.** The leaf pipeline model of energy fluxes through PSII of excited cross sections (CS) of investigated three sugar beet cultivars (Viola, Jaromir, and Pulitzer) from September to November. Each relative value of the measured parameters is the mean ( $n = 60$ ) and each arrow's width corresponds to the flux's intensity. Yellow arrow—ABS/CS, absorption flux per CS approximated; green arrow—TR/CS, trapped energy flux per CS; red arrow—ET/CS, electron transport flux per CS; blue arrow—DI/CS, dissipated energy flux per CS; circles inscribed in squares—RC/CS, % of active/inactive reaction centers. White circles inscribed in squares represent reduced  $Q_A$  reaction centers (active), black (or orange) circles represent non-reduced  $Q_A$  reaction centers (inactive), 100% of the active reaction centers responded with the highest mean value observed in the control conditions. Means followed by the same letter for each parameter are not significantly different from each other using the Fisher LSD test ( $P < 0.05$ ). Letters are inscribed into arrows, except for RC/CS, where they are placed in a box in the bottom right corner of the square with circles.

of intracellular  $\text{CO}_2$  and stomatal conductance were measured in October for all beet cultivars, but mentioned parameters increased significantly in November (Fig. 6B, D).

## Results analysis for the tested beet varieties in individual months

Analyzing the principal components allowed us to distinguish groups of variables dominating the physiological response of sugar beets in the examined months of the growing season (Fig. 7). The best gas exchange in sugar beet leaves was observed in September which was crucial together with glucose content for separate grouping of tested plants in this month. In October, the light phase of photosynthesis reached the optimal level, and the sugar content in the roots was the highest. In November, the content of sugar and flavonoids in the leaves increased (Fig. 7). Simultaneously, the PCA analysis confirmed that the *Viola* variety aged significantly slower than *Pulitzer* and *Jaromir* (Fig. 7). A strong negative correlation was also detected between the intensity of CLS infection and the sugar content in the root. Moreover, the strongest positive correlation with the sugar content in sugar beet roots was demonstrated for the results of Green LAI and electron transport in the light phase of photosynthesis (Fig. S2).

## Results analysis for individual months without distinction of the beet cultivars

When considering physiological changes in sugar beets, regardless of the cultivar, many significant relationships were observed (Fig. 8). The highest sugar content in the root was measured in October, while the value was significantly lower in November. However, most of the sugars in beetroot leaves were found in November. In

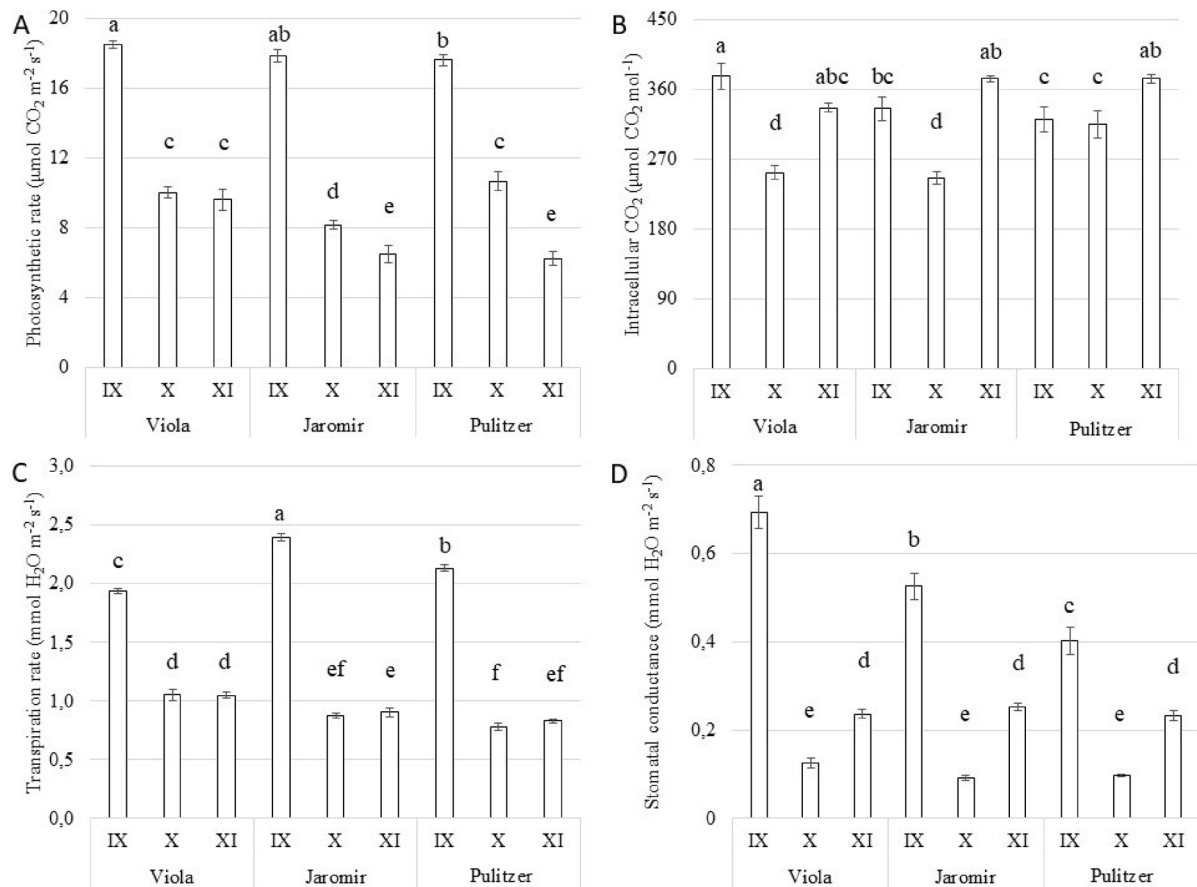


**Fig. 6.**  $\text{CO}_2$  assimilation (A), intracellular  $\text{CO}_2$  concentration (B), transpiration (C), and stomatal conductance (D) in Viola, Jaromir, and Pulitzer cultivars of sugar beet from September (IX) to November (XI). Presented values are means  $\pm$  SE ( $n=60$ ). Lowercase letters describe statistical significance (ANOVA, LSD test).

turn, the highest accumulations of fat and fiber in beetroot leaves were recorded in October. In October, beetroot leaves contained the most chlorophyll, which was associated with the highest PSII efficiency. The lowest values of these two parameters were measured in September. Beet gas exchange had the highest rate in September. The content of flavonols and anthocyanins in beetroot leaves increased significantly as they aged (Fig. 8).

## Discussion

In this experiment, field trials of three cultivars of sugar beet (Viola, Jaromir, Pulitzer) were conducted between September and November using a wide range of in vivo, biochemical, and remote sensing methods. The crucial part of the experiment was related to the occurrence of Cercospora leaf spots (CLS) related to *Cercospora beticola* infection in September, resulting in significant plantation damage. This observation was confirmed in the field and remotely using multispectral satellite imaging. Moreover, these data were crucial to understanding the monthly changes dynamics in other measured parameters, which clearly indicate a short recovery phase after infection due to an increase of Green LAI indices. Previous studies have indicated the successful use of remote sensing to determine the change in plant-infected canopy caused by CLS disease of sugar beets using vegetation indices like NDVI<sup>22</sup>. The data retrieved from multispectral imaging could not detect infection without field inspection. However, those became valuable tools to track its progression and recovery<sup>23</sup>. Despite this fact, there is more and more interest in the use of multispectral images to differentiate diseases of sugar beet and many other plant species<sup>24–27</sup>.

In vivo measurements were particularly associated with photosynthesis-related parameters widely used to assess cultivar-specific behavior under variable environmental conditions and biotic and abiotic stresses<sup>28–30</sup>. There is a lot of research on photosynthesis in vivo measurement for sugar beet, however, those are related to the pot experiments<sup>20,31,32</sup> or to measurements at specific dates or at the rapid growth stage at the beginning of the season in most cases<sup>33–35</sup>. On the other hand, there is a gap in field intra-seasonal measurements, especially those focused on last months of growing<sup>30,36</sup>.

In our study, the analyzed pigment contents showed the same seasonal pattern for the three investigated sugar beet cultivars. Chlorophyll content was the lowest in September, and significantly higher values were found for subsequent measurements. Flavonols increased their values from September to November, while anthocyanin content was at the same level in September and October, with the following increase in November. Yetik et al.<sup>37</sup>

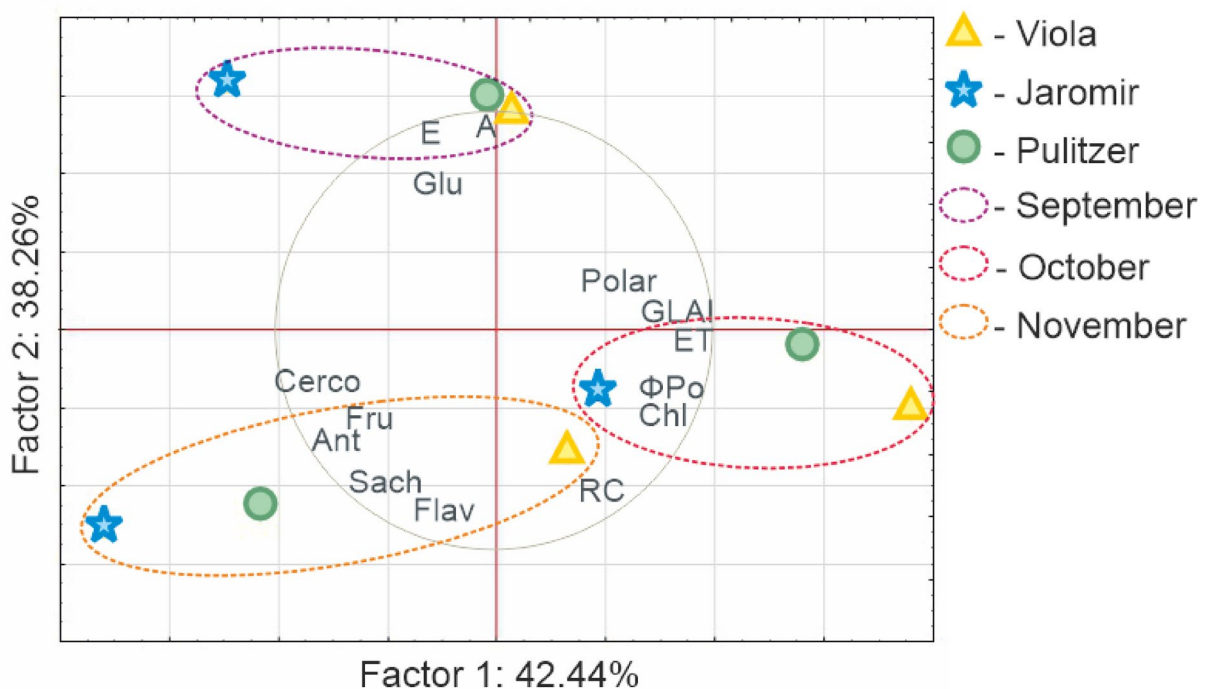


**Fig. 7.** Principal component analysis (PCA) presenting the relationships between selected sugar beet physiological parameters depending on the cultivar (Viola—yellow triangle, Jaromir—blue star, and Pulitzer—green circle) and month of the growing season. Abbreviations: A—CO<sub>2</sub> assimilation, E—transpiration rate, Ant—anthocyanins content, Chl—chlorophyll content, Flav—flavonol content, Cerco—severity of CLS infection, GLAI—Green Leaf Area Index, Glu—glucose content in leaves, Fru—fructose content in leaves, Sach—sucrose content in leaves, Polar—polarisation (root sugar content),  $\phi P_0$ —maximum quantum yield of photosystem II, ET—electron transport flux per leaf excited cross-section, RC—% of active reaction centers per leaf cross-section.

found a decrease in relative chlorophyll content in sugar beet leaves between 120 and 135 days after sowing, which relates to September, irrespectively on water treatment. Moreover, the same authors found that the rate of decrease could vary between growing seasons. This observation is contrast to the results obtained in the current study. However, there was a difference associated with CLS infection, which could trigger the recovery process afterward. Considering anthocyanins content, it was previously reported that this relative value could be an indicator of leaf senescence<sup>38</sup> or abiotic stress<sup>39,40</sup>. Especially the first mentioned phenomenon it is with an agreement to obtained results as the significant increase was found in the harvest month (November). It was suggested by Rusinowski et al.<sup>41</sup>, that considering the relative pigment contents and derivative from this measurement, which is Nitrogen Balance Index (NBI), form all of them NBI, which is a proximate indicator of C: N allocation changes could be a more valuable tool for estimating the rate of senescence than the relative chlorophyll content as proposed by others<sup>38,42,43</sup>.

The photosynthesis rate measured during this experiment decreased starting from September, with the highest drop between September and October; however, for the Viola variety, it remained unchanged between November and October. Despite this, Jaromir experienced a higher decrease between the first and the second measurements. On the one hand, those findings are in agreement with the report by Barrat et al.<sup>30</sup>, (ca. 140 DAS as a starting point in this experiment). On the other hand,  $g_s$  registered by Barrat et al.<sup>30</sup>, in 2018 exhibit the same significant decrease of values between 120 and 180 DAS, while in 2019 the less pronounced decrease was found. However, fluctuation of this parameter as in this experiment was reported at the end of the season. This indicates that reported fluctuation in  $g_s$ , with high probability, is associated with the season specificity or could be related to the recovery process after CLS. Fitters et al.<sup>44</sup> reported the seasonal pattern of changes for stomatal conductance for sugar beet. It was shown that values at the beginning of leaf development are low until it achieves pick in the ca. 1/3rd of the leaf lifespan, which is followed by a continuous decrease<sup>45</sup>. Considering the above and visible symptoms of leaves regrowing after CLS infection in the field, it could be hypothesized that a decrease of stomatal conductance followed by an increase was rather associated with extensive necrosis and re-growth in October. The chlorophyll content reaching stability in October may confirm this assumption.

The most common parameter obtained from prompt chlorophyll *a* fluorescence measurement is Fv/Fm (or  $\phi P_0$ ). As could be expected, its highest value was recorded for October, while similar lower values were found for September and November, especially considering Jaromir and Pulitzer cultivars. Viola was less susceptible to the fluorescence parameters decrease between October and November. This parameter ( $\phi P_0$ ) was previously used to assess sugar beet response to different biotic and abiotic stress<sup>46–48</sup>, and in healthy plants should have a value

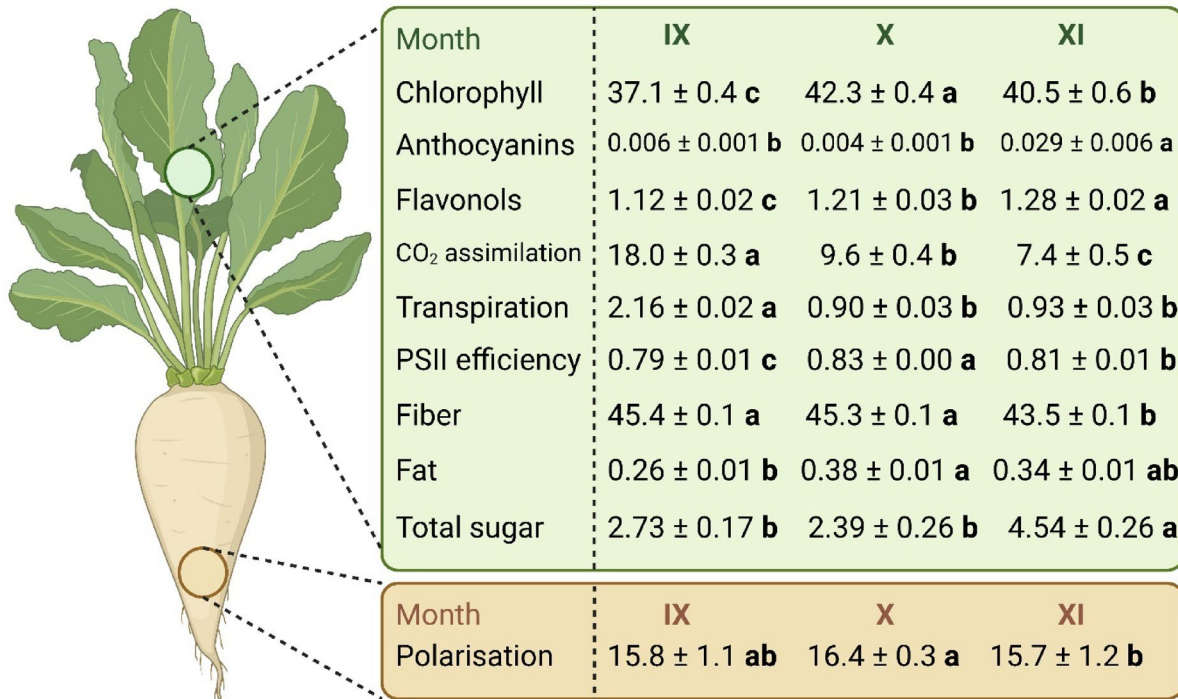


**Fig. 8.** Model of monthly changes in selected physiological parameters as an average of the results for the three cultivars. The described changes concern pigment contents in leaves (chlorophyll, flavonols and anthocyanins), gas exchange (transpiration and CO<sub>2</sub> assimilation), maximum quantum efficiency of photosystem II (PSII efficiency), chemical composition of leaves (fat and fiber) and sugar balance in the leaf: root system (the sum of glucose, fructose and sucrose content in the leaves (total sugar) and sugars in the root (polarization)). Lowercase letters describe statistical significance in a row (ANOVA, LSD test). Created in BioRender. Sitko, K. (2025) <https://BioRender.com/z52p437>.

around 0.80–0.83<sup>38</sup>. Considering the results obtained, all of the values for this indicator were within the range of healthy plants; despite this fact, they varied at measuring months.

Most of the research on the chlorophyll fluorescence of sugar beet focuses on different applications of abiotic stress factors e.g., nutrient deficiency or herbicides. In those cases, variable relative chlorophyll fluorescence ( $\Delta V$ ) shows efficiency reduction on the K-J-I phase in electron transient<sup>35,47</sup>. In our research, infested leaves in September exhibit behavior similar to that found in the above research; however, considering November measurements, an increase in efficiency was found in the J-I-P phase. This, considering results obtained from chlorophyll fluorescence parameters ( $\varphi R_0$ ,  $\delta R_0$ ), suggests that despite visible symptoms of senescence in other measurements and/or parameters, the light-dependent photosynthesis phase is the most efficient in reduction of the end acceptors at the PSI acceptor side. On the one hand, Sitko et al.<sup>38</sup> reported that during leaf lifespan, there is a decrease in PSI-related parameters for grapevine leaves, and this observation was also confirmed by others for other plant species<sup>49</sup>. On the other hand, such relationships were not found in this report. A possible explanation could be related to cyclic electron flow around PSI (CEF-PSI), which is associated with Non-photochemical quenching (NPQ) as it requires a pH gradient across the thylakoid membranes. The acidification of the thylakoid lumen is driven by CEF-PSI<sup>50</sup>. The validity of this observation in the current work could be supported by the report presented by Kotakis et al.<sup>18</sup>, who indicate that local ATP needs in the degrading chloroplast, with its inhibited linear electron flow, might still be met by enhanced alternative electron routes around PSI, i.e., CEF-PSI. Even though in obtained data for phenomenological energy fluxes (ABS/CS, TR/CS, ET/CS, RC/CS, and DI/CS), there was a decrease of parameters preferably due to ongoing senescence visible in November measurements. Above mechanism still could be the case in a situation where Rubisco was rapidly degraded, while leaf absorbance decreases at a much slower rate than chlorophyll concentration<sup>18</sup>.

In general, gas exchange constantly decreased since September at different rates for investigated varieties, while chlorophyll content and fluorescence measurement showed fluctuations indicating recovery of light-dependent photosynthesis phase after CLS infection followed by senescence. As processes involved in this behavior could be similar for investigated varieties, the range of recovery and rate of senescence vary. It appears that the *Viola* cultivar was less susceptible to the reported fluctuations, which could be driven by resilience to CLS infection, faster and more efficient recovery, or delayed senescence when compared to other investigated varieties. Considering Green LAI data, the efficient recovery after CLS seems to be the most relevant.

Leaf composition, especially different hydrocarbon content, was found to be inconsistent between investigated cultivars. The only consistent part relates to the sucrose content, which increased in the last measuring date and was 5-, 6-, and 3 times higher in September when compared to November for *Viola*, *Jaromir*, and *Pulitzer*,

respectively. Giaquinta<sup>19</sup> found using the same method on leaf lifespan (up to 80 days) that at the beginning<sup>14</sup>, C is mostly associated with glucose and fructose, while at the end of the leaf lifespan, the Sucrose accumulation increases, suggesting a strong negative correlation, between this two groups of sugars. Those observations are mainly associated with the activity of sucrose phosphate synthase (SPS), sucrose synthase (SS), and invertase (INV), which are sucrose metabolism-related enzymes<sup>51</sup>. The observed significantly higher accumulation of sucrose in this experiment could be related to both the physiological senescence of the leaves 58 and/or to low night temperature in November, which could lead to reduced sucrose output from leaves to roots<sup>35</sup>. The total carbohydrate content in leaves showed a different pattern in the *Viola* cultivar than in others. For *Viola*, the total carbohydrate content increases with each sampling campaign, while for *Jaromir* and *Pulitzer*, it decreases in October when compared to September, while it increases significantly in November to attain values higher than in September. Watson and Watson<sup>52</sup> reported that total carbohydrate contents in sugar beet were generally higher in young leaves than in old leaves, suggesting a decrease in total carbohydrate content over the leaf lifespan. However, their experiment included an infestation of sugar beet with a mosaic virus, which reverted this behavior. Considering the above and the obtained results in this experiment, it could be suggested that CLS could impact the carbohydrate content and the balance of different compounds associated with them.

Sugar content in roots was in a similar range as found in the literature data<sup>45,48,53</sup>. Ebmeyer et al.<sup>45</sup> reported that the level of sugar content in the root strongly depends on the environment and use of genotype. Hoffman and Kluge-Severin<sup>54</sup> reported that in spring-sown sugar beet (as in this experiment), sugar content continuously increases in below-ground organs until harvest; however, considering autumn-sown sugar beet, the concentration of sugar decreases between December and June. On the one hand, Spring sown cultivars did not fully relate to data obtained in this experiment, especially for November; on the other hand, late harvest (November) and post-CLS infection recovery could affect sugar content in November, which suggests harvesting earlier in that particular condition to obtain the most desirable product.

Based on the results presented in this work, we can conclude that the efficiencies of CO<sub>2</sub> and solar energy assimilation are not correlated in time and space in beetroot, which, in the context of autumn leaf regeneration, may also indicate to farmers to harvest earlier. Moreover, selected cultivars may demonstrate higher (*Viola*) or lower (*Jaromir*) resistance to CLS, which may also be influenced by environmental variables, such as the heterogeneous presence of fungal spores in the soil. The experiment was conducted during a single growing season, which is a certain limitation, the consequence of which is a strong suggestion for further research. This is especially true since the experimental introduction of a variety highly susceptible to CLS into a field cultivation is not acceptable due to the risk of spreading the pathogen over a large area. The regeneration of leaves after CLS infection in beetroot seems to be independent of the sugar accumulated in the root. Sugar beetroot varieties are characterized by different strategies for managing sugar production and relocation, which can be used by farmers to avoid the effects of CLS infection. Furthermore, the use of the Green LAI indicator in monitoring not only CLS but also other fungal infections in crops seems to be a significant innovation in large-scale agriculture.

## Materials and methods

### Plant material and growing conditions

Three varieties of sugar beet were used in the research: *Viola*, *Jaromir*, and *Pulitzer* (produced by KWS Polska LLC, KHBC LLC, and Strube Polska LLC, respectively). All producers declared increased resistance of the above-mentioned sugar beet varieties to *Cercospora beticola*. Due to the impossibility of introducing a variety highly susceptible to *C. beticola* into the field cultivation, and the lack of varieties completely resistant to the pathogen, experiments were conducted on varieties that clearly differed in their physiological response to CLS. The arable field with an area of approximately 83 ha was located in the village of Polanowice (Kuyavian-Pomeranian Voivodeship), in central Poland. Each tested sugar beet variety occupied an area in the field in the form of a strip with dimensions of approximately 50 × 800 m and an area of 4 ha. The soils of this region are characterized by high fertility; data on soil properties are presented in Table 2. The average annual atmospheric precipitation is 669 mm, and the average temperature oscillates around 8.9 °C.

### Soil physico-chemical analyses

Six soil samples (0–20 cm depth) were collected randomly from the field. Soil samples were mixed, air-dried, and sieved through 2 mm and 0.25 mm sieve for further analysis. Soil (2 mm) pH was measured in 1 M KCl (ratio 1:2.5 m/v) with the electrode (OSH 10 – 0, METRON, Poland) and pH-meter (CPC-551, Elmetron, Poland) at 20 °C according to the Polish standard PN-ISO 11265:1997<sup>55</sup>. Soil (2 mm) texture was determined according to the Polish standard PNR-04032:1998, using the hydrometric method. Soil organic matter (SOM) content was measured by loss on ignition as follows: 5 g of air-dry soil was dried at 105 °C for 24 h and then treated by 550 °C for four hours. Organic carbon content was determined using Thiurin method. For the determination of the pseudo-total concentrations of Cd, Pb, and Zn soil samples (0.25 mm) were digested with aqua regia<sup>56</sup> and analyzed using flame atomic absorption spectrometry (SpektrAA 300, Varian INC., USA). The bioavailable fraction of Pb, Cd, and Zn were analyzed in the soil after extraction with 0.01 M CaCl<sub>2</sub> according to the method described by Pogrzeba et al.<sup>57</sup> and measured using an atomic absorption spectrometer (SpektrAA 300, Varian INC., USA). The dry combustion method<sup>58</sup> was used for the determination of total N concentration in the soil, while the total concentration of P, K, Ca and Mg were analyzed in the previously digested samples using the Inductively Coupled Plasma Optical Emission Spectrometry method (ICP-OES, Liberty 220, Varian, USA). The NO<sub>3</sub>, NO<sub>2</sub> and NH<sub>4</sub><sup>+</sup> content in the soil was determined using Kjeldahl method. The concentrations of available phosphorus and available potassium were determined according to the method described by Egnér et al.<sup>59</sup>.

Parameter	Mean $\pm$ SE
pH (H <sub>2</sub> O)	7.36 $\pm$ 0.07
pH (KCl)	7.12 $\pm$ 0.01
EC (μS/cm)	234 $\pm$ 4
OM (%)	6.24 $\pm$ 0.10
C-org.	2.24 $\pm$ 0.36
N <sub>tot</sub> (%)	0.22 $\pm$ 0.01
Zn <sub>av</sub> (mg/kg)	0.20 $\pm$ 0.03
Pb <sub>av</sub> (mg/kg)	BDL
Cd <sub>av</sub> (mg/kg)	BDL
Zn <sub>tot</sub> (mg/kg)	29.2 $\pm$ 0.3
Pb <sub>tot</sub> (mg/kg)	7.5 $\pm$ 0.2
Cd <sub>tot</sub> (mg/kg)	0.07 $\pm$ 0.02
NO <sub>3</sub>	12.5 $\pm$ 0.3
NO <sub>2</sub>	0.1 $\pm$ 0.0
NH <sub>4</sub>	22.6 $\pm$ 0.1
P (mg P <sub>2</sub> O <sub>5</sub> /100 g)	44.7 $\pm$ 1.1
K (mg K <sub>2</sub> O/100 g)	86.7 $\pm$ 2.2
P (mg/kg)	680 $\pm$ 15
K (mg/kg)	3470 $\pm$ 10
Ca (mg/kg)	3920 $\pm$ 130
Mg (mg/kg)	2180 $\pm$ 30

**Table 2.** Field soil characteristics. Data are means  $\pm$  SE ( $n = 6$ ). Abbreviations: EC—electrical conductivity; OM—soil organic matter content; X<sub>av</sub>—photo-available fraction of metal X in soil; X<sub>tot</sub>—pseudo-total content of metal X in soil; C-org—organic carbon in soil.

### Severity of *Cercospora beticola* infection evaluation

The CLS disease incidence and severity were assessed on plants from the three middle rows in each block separately, according to the CERCOPRI Standard scale<sup>60</sup>. This is a 10-point scale, where 0 indicates no disease symptoms, while 9 indicates complete destruction of leaves and the appearance of new leaves produced by the plant. The incidence and severity of CLS were assessed on the day of the sugar beet harvest. Each replicate was assessed on ten consecutive plants from each row.

### Satellite data acquisition and processing

To determine spatial changes in Green LAI for experimental plots on the field, bounding box for each were defined with margin for exclude mixels on the field edge. Using EO Browser from Sentinel-hub<sup>61</sup> (<https://apps.sentinel-hub.com/eo-browser/>), dates were selected which fulfill the following requirements: were close to the in vivo parameters measurement dates, there was no cloud over the field, data were available due to satellite acquisition. L1 C/L2 A layers were analyzed in terms of desired indices at dates 08.08.2022, 24.09.2022, 12.10.2022 and 08.11.2022 to track the spatial changes in *C. beticola* infection progression and recovery. Spatial map for Green LAI were generated using Quick Zone Software (developed and maintain by QZ Solutions) based on Sentinel-2 data and provided plots bounding box. Moreover, the spatial distribution of LAI for the same plots was analyzed using a custom script from sentinel-hub<sup>62</sup> (<https://custom-scripts.sentinel-hub.com/custom-scripts/sentinel-2/lai/>). Average values of indices for each plot separately were used for further analysis.

### Determination of sugar beet polarization by cold fume hood with aluminum sulfate clarification

The polarization of sugar beet was determined by the polarimetric method GS6-3 (1994) according to ICUMSA analytical regulations. This method involves measuring the rotation angle of the sucrose polarization plane in a polarimeter in sugar beet pulp prepared by cold fume slurry using aluminum sulfate as a clarifying agent. For the determinations, six representative beets of each variety were collected from the field; the research samples were combined with material from two beets per sample.

A sample of  $26 \pm 0.05$  g of freshly prepared or frozen beet pulp was weighed and fumigated in a fixed volume of  $177 \pm 0.35$  ml of an aqueous solution of aluminum sulfate. Using a mixer, a “semi-normal sugar solution” was obtained; then, after filtration, the sugar content in the clear filtrate was determined polarimetrically.

An MCP 250 (Anton Paar) was used for analysis. The following conditions were used: wavelength 589 nm, reading at 20.0 °C in a 200 mm long tube.

### Gas exchange, chlorophyll fluorescence, and plant pigment content measurements

Gas exchange, chlorophyll fluorescence, and plant pigment content measurements were performed on the fully developed leaf located in the center of the leaf rosette. The leaves selected for measurement were as representative

as possible of the CLS infection degree of a given sugar beet variety. The degree of disease infection of a given variety was determined each time before the measurements of physiological parameters.

Gas exchange measurements were performed with an infra-red gas analyzer (LCpro SD, ADC Bioscientific UK). The measurements of saturated photosynthesis rate (A), transpiration rate (E), and stomatal conductance (gs) were done. Each leaf was kept in the chamber, until reading stabilization (3–5 min). The LCpro SD was equipped with a narrow chamber (580 mm<sup>2</sup> set to 22 °C, PAR = 1000 µmol E m<sup>-2</sup> s<sup>-1</sup>, with ambient CO<sub>2</sub> levels, as described previously by Rusinowski et al.<sup>39</sup>. Measurements were made on twelve leaves per beet cultivar, on each leaf being measured five times ( $n = 60$ ).

Chlorophyll *a* fluorescence measurements were done using Handy Plant Efficiency Analyzer, (Hansatech Instruments Ltd., UK) on the previously dark-adapted leaves using specially dedicated leaf clips (LC, Hansatech Instruments Ltd., UK) for 25 min. The measurement parameters were set in the fluorimeter according to Rusinowski et al.<sup>39</sup>. For each of the plot, twenty leaves were measured, with three clips on each ( $n = 60$ ). An increase in the fluorescence of chlorophyll *a* (prompt chlorophyll fluorescence) was shown as a typical OJIP transient since fluorescence was measured at the time of 1 s on a logarithmic scale<sup>63</sup>. Meaning of each obtained band (O- J- I- P-band), as well as phases (between bands), was described previously<sup>38,64,65</sup>. JIP-test parameters resulting from obtained fluorescence transient curves were calculated according to Strasser et al.<sup>63</sup>. O-band corresponds to minimal fluorescence (Fo), K-band corresponds to fluorescence yield at 0.0003 s, J-band to fluorescence yield at 0.002 s, I-band to fluorescence yield at 0.01 s, while P-band corresponds to maximal fluorescence yield (Fm).

Relative chlorophyll content, anthocyanin, and flavonol pigments (relative units) were measured using a plant pigment content meter (Dualex Scientific+, Force-A, France). Additionally, the Dualex device provided a Nitrogen Balance Index (NBI = Chl/Flav). For each of the plot, sixty measurements were done.

### Determination of total fat, fiber, and carbohydrates content in sugar beet leaves

Measurements were performed according to the methods described in Baryga et al.<sup>15</sup>. For the determinations, six representative beets of each variety were collected from the field; the research samples were combined with material from two beets per sample. The content of essential nutrients in the analyzed sample was determined by AOAC methods<sup>66</sup>. Protein content ( $N \times 5.7$ ) was assessed by Kjeldahl's method (AOAC 920.87), applying extraction unit Kjeltec 2200 (Foss, Denmark), total carbohydrate content was evaluated following AOAC 974.06, fat according to Soxhlet's method AOAC 953.38, applying the extractor Soxtec Avanti 2055 (Foss, Denmark), and ash by gravimetric method (AOAC 930.05). The content of non-starch polysaccharides, i.e., total, soluble, and insoluble dietary fiber, was determined by method 32 – 07, while reducing sugars were determined according to method 906.01 AOAC<sup>66</sup>. Each of the above determinations was performed in at least two replicates.

### Statistical analyses and software

The results are shown as the means  $\pm$  SE. In order to enable comparison of the significance of differences between different beet varieties in different months, a one-way ANOVA and a post hoc Fisher LSD test was used ( $p < 0.05$ ). Principal Component Analysis was performed to investigate the relationship between the tested parameters for different beet varieties in different months. The statistical analysis was performed using Statistica v.13.1 software (Dell Inc., Austin, TX, USA). The pipeline models of energy fluxes through the leaf's cross-section (Fig. 5) were done using CorelDRAWX6 (Corel Corp., Ottawa, ON, Canada). Figure 8 was created in BioRender by Krzysztof Sitko (<https://BioRender.com/z52p437>).

### Data availability

The datasets used and/or analysed during the current study available from the corresponding author on reasonable request.

Received: 9 December 2024; Accepted: 23 May 2025

Published online: 03 June 2025

### References

1. McGrath, J. M. & Townsend, B. J. Sugar beet, energy beet, and industrial beet. In *Industrial Crops: Breeding for BioEnergy and Bioproducts* (eds Cruz, V. M. V. & Dierig, D. A.) 81–99 (Springer, 2015). [https://doi.org/10.1007/978-1-4939-1447-0\\_5](https://doi.org/10.1007/978-1-4939-1447-0_5).
2. Geng, G. & Yang, J. Sugar beet production and industry in China. *Sugar Tech.* **17**, 13–21 (2015).
3. Tan, W., Li, K., Liu, D. & Xing, W. Cercospora leaf spot disease of sugar beet. *Plant Signal. Behav.* **18**, 2214765 (2023).
4. Poleć, B. & Baryga, A. Methanový fermentační proces Cukrovarnických Odpadů. *LISTY CUKROVARNICKÉ ŘEPARSKÉ* **132**, 246–252 (2016).
5. Poleć, B., Baryga, A., Szymański, T. & Małczak, E. Methanová fermentace Vyslažených Cukrovarnických Řízků s Přidáním Hovězí Kejdy. *LISTY CUKROVARNICKÉ ŘEPARSKÉ* **133**, 352–359 (2017).
6. Baryga, A., Poleć, B. & Klasa, A. Quality of sugar beets under the effects of digestate application to the soil. *Processes* **8**, 1402 (2020).
7. Scott, R. K. & Jaggard, K. W. Crop physiology and agronomy. In *The Sugar Beet Crop* (eds Cooke, D. A. & Scott, R. K.) 179–237 (Springer Netherlands, 1993). [https://doi.org/10.1007/978-94-009-0373-9\\_6](https://doi.org/10.1007/978-94-009-0373-9_6).
8. Clover, G. R. G., Azam-Ali, S. N., Jaggard, K. W. & Smith, H. G. The effects of beet yellows virus on the growth and physiology of sugar beet (*Beta vulgaris*). *Plant. Pathol.* **48**, 129–138 (1999).
9. Clover, G. R. G., Smith, H. G., Azam-Ali, S. N. & Jaggard, K. W. The effects of drought on sugar beet growth in isolation and in combination with beet yellows virus infection. *J. Agric. Sci.* **133**, 251–261 (1999).
10. Kiskini, A., Vissers, A., Vinczen, J. P., Gruppen, H. & Wierenga, P. A. Effect of plant age on the quantity and quality of proteins extracted from sugar beet (*Beta vulgaris* L.) leaves. *J. Agric. Food Chem.* **64**, 8305–8314 (2016).
11. Milford, G. F. J. et al. An analysis of leaf growth in sugar beet. *Ann. Appl. Biol.* **107**, 335–347 (1985).
12. Milford, G. F. J., Pocock, T. O. & Riley, J. An analysis of leaf growth in sugar beet. *Ann. Appl. Biol.* **106**, 173–185 (1985).
13. Holtschulte, B. *Cercospora beticola*: World-Wide Distribution and Incidence.

14. Piszczeck, J. Rizomania—najgroźniejsza Choroba Wirusowa Buraka Cukrowego. *Poradnik Plantatora Buraka Cukrowego*. **3**, 10–12 (2000).
15. Daub, M. E. & Ehrenshaft, M. The photoactivated cercospora toxin cercosporin: contributions to plant disease and fundamental biology. *Annu. Rev. Phytopathol.* **38**, 461–490 (2000).
16. Rangel, L. I. et al. *Cercospora beticola*: the intoxicating lifestyle of the leaf spot pathogen of sugar beet. *Mol. Plant Pathol.* **21**, 1020–1041 (2020).
17. Ebert, M. K. et al. Identification and characterization of *Cercospora beticola* necrosis-inducing effector CbNip1. *Mol. Plant Pathol.* **22**, 301–316 (2021).
18. Kotakis, C., Kyzeridou, A. & Manetas, Y. Photosynthetic electron flow during leaf senescence: evidence for a Preferential maintenance of photosystem I activity and increased Cyclic electron flow. *Photosynt* **52**, 413–420 (2014).
19. Giaquinta, R. T. Sucrose translocation and storage in the sugar beet 1. *Plant Physiol.* **63**, 828–832 (1979).
20. Wu, Z. et al. Responses of photosynthetic performance of sugar beet varieties to foliar boron spraying. *Sugar Tech.* **23**, 1332–1339 (2021).
21. Kinić, A., Piszczeck, J., Miziniak, W. & Sitarski, A. Impact of the variety and severity of *Cercospora beticola* infection on the qualitative and quantitative parameters of sugar beet yields. *Pol. J. Agron.* 29–37. <https://doi.org/10.26114/pja.iung.410.2020.41.04> (2020).
22. Yamati, F. R. I., Heim, R. H., Günder, M., Gajda, W. & Mahlein, A. K. Image-to-image translation for satellite and UAV remote sensing: a use case for *Cercospora* Leaf Spot monitoring on sugar beet. In *IEEE International Workshop on Metrology for Agriculture and Forestry (MetroAgriFor)* 783–787 (2023). <https://doi.org/10.1109/MetroAgriFor58484.2023.10424276>
23. Lowe, A., Harrison, N. & French, A. P. Hyperspectral image analysis techniques for the detection and classification of the early onset of plant disease and stress. *Plant. Methods* **13**, 80 (2017).
24. Zhang, M., Qin, Z., Liu, X. & Ustin, S. L. Detection of stress in tomatoes induced by late blight disease in California, USA, using hyperspectral remote sensing. *Int. J. Appl. Earth Obs. Geoinf.* **4**, 295–310 (2003).
25. Mahlein, A. K., Steiner, U., Dehne, H. W. & Oerke, E. C. Spectral signatures of sugar beet leaves for the detection and differentiation of diseases. *Precis. Agric.* **11**, 413–431 (2010).
26. Mahlein, A. K., Steiner, U., Hillnhütter, C., Dehne, H. W. & Oerke, E. C. Hyperspectral imaging for small-scale analysis of symptoms caused by different sugar beet diseases. *Plant. Methods* **8**, 3 (2012).
27. Tomaszewski, M., Nalepa, J., Moliszewska, E., Ruszczak, B. & Smykala, K. Early detection of *Solanum lycopersicum* diseases from temporally-aggregated hyperspectral measurements using machine learning. *Sci. Rep.* **13**, 7671 (2023).
28. Chaerle, L., Hagenbeek, D., De Bruyne, E. & Van Der Straeten, D. Chlorophyll fluorescence imaging for disease-resistance screening of sugar beet. *Plant. Cell. Tiss. Organ. Cult.* **91**, 97–106 (2007).
29. Abbas, F., Al-Jbawi, E. & Ibrahim, M. Growth and chlorophyll fluorescence under salinity stress in sugar beet (*Beta vulgaris* L.). *Int. J. Environ.* **3**, 1–9 (2014).
30. Barratt, G. E., Murchie, E. H. & Sparkes, D. L. Water use efficiency responses to fluctuating soil water availability in contrasting commercial sugar beet varieties. *Front. Plant. Sci.* **14** (2023).
31. Shaw, B., Thomas, T. H. & Cooke, D. T. Responses of sugar beet (*Beta vulgaris* L.) to drought and nutrient deficiency stress. *Plant. Growth Regul.* **37**, 77–83 (2002).
32. Jamil, M., Rehman, S., Rha, E. S., Salinity effect on plant growth & PSII photochemistry and chlorophyll content in sugar beet (*Beta vulgaris* L.) and cabbage (*Brassica oleracea capitata* L.).
33. Libutti, A., Trotta, V. & Rivelli, A. R. Biochar, vermicompost, and compost as soil organic amendments: influence on growth parameters, nitrate and chlorophyll content of Swiss chard (*Beta vulgaris* L. Var. *cycla*). *Agronomy* **10**, 346 (2020).
34. Elsayed, S. et al. Estimating chlorophyll content, production, and quality of sugar beet under various nitrogen levels using machine learning models and novel spectral indices. *Agronomy* **13**, 2743 (2023).
35. Wang, Y. et al. New insight into the pigment composition and molecular mechanism of flower coloration in tulip (*Tulipa gesneriana* L.) cultivars with various petal colors. *Plant Sci.* **317**, 111193 (2022).
36. Wang, N. et al. Effects of irrigation and nitrogen on chlorophyll content, dry matter and nitrogen accumulation in sugar beet (*Beta vulgaris* L.). *Sci. Rep.* **11**, 16651 (2021).
37. Yetik, A. K. & Candoğan, B. N. Chlorophyll response to water stress and the potential of using crop water stress index in sugar beet farming. *Sugar Tech.* **25**, 57–68 (2023).
38. Sitko, K. et al. Influence of short-term macronutrient deprivation in maize on photosynthetic characteristics, transpiration and pigment content. *Sci. Rep.* **9**, 14181 (2019).
39. Rusinowski, S. et al. How autochthonous microorganisms influence physiological status of *Zea mays* L. cultivated on heavy metal contaminated soils? *Environ. Sci. Pollut. Res.* **26**, 4746–4763 (2019).
40. Sitko, K. et al. Development and aging of photosynthetic apparatus of *Vitis vinifera* L. during growing season. *Photosyntetica* **57**, 1–8 (2019).
41. Rusinowski, S. et al. New *Miscanthus* hybrids cultivated at a Polish metal-contaminated site demonstrate high stomatal regulation and reduced shoot Pb and Cd concentrations. *Environ. Pollut.* **252**, 1377–1387 (2019).
42. Bury, M. et al. Physiological status and biomass yield of *Sida hermaphrodita* (L.) Rusby cultivated on two distinct marginal lands in Southern and Northern Poland. *Ind. Crops Prod.* **167**, 113502 (2021).
43. Gieron, Ź. et al. Ecophysiology of *Arabidopsis arenosa*, a new hyperaccumulator of Cd and Zn. *J. Hazard. Mater.* **412**, 125052 (2021).
44. Fitters, T. F. J., Bussell, J. S., Mooney, S. J. & Sparkes, D. L. Assessing water uptake in sugar beet (*Beta vulgaris*) under different watering regimes. *Environ. Exp. Bot.* **144**, 61–67 (2017).
45. Ebmeyer, H., Fiedler-Wiechers, K. & Hoffmann, C. M. Drought tolerance of sugar beet—Evaluation of genotypic differences in yield potential and yield stability under varying environmental conditions. *Eur. J. Agron.* **125**, 12626 (2021).
46. Islam, M. J., Kim, J. W., Begum, M. K., Sohel, M. A. T. & Lim, Y. S. Physiological and biochemical changes in sugar beet seedlings to confer stress adaptability under drought condition. *Plants* **9**, 1511 (2020).
47. Song, X. et al. Effect of Boron deficiency on the photosynthetic performance of sugar beet cultivars with contrasting Boron efficiencies. *Front. Plant. Sci.* **13** (2023).
48. Sacristán-Pérez-Minayo, G., López-Robles, D. J. & Rad, C. & Miranda-Barroso, L. Microbial inoculation for productivity improvements and potential biological control in sugar beet crops. *Front. Plant. Sci.* **11** (2020).
49. Viljevac Vuletić, M. & Španić, V. Special issue in honour of prof. Reto J. Strasser - Characterization of photosynthetic performance during natural leaf senescence in winter wheat: Multivariate analysis as a tool for phenotypic characterization. *Photosynt* **58**, 301–313 (2020).
50. Miyake, C. et al. Effects of light intensity on Cyclic Electron flow around PSI and its relationship to Non-photochemical quenching of Chl fluorescence in tobacco leaves. *Plant Cell Physiol.* **46**, 1819–1830 (2005).
51. Shao, K. et al. Sucrose metabolism enzymes affect sucrose content rather than root weight in sugar beet (*Beta vulgaris*) at different growth stages. *Sugar Tech.* **22**, 504–517 (2020).
52. Watson, M. A. & Watson, D. J. The effect of infection with beet yellows and beet mosaic viruses on the carbohydrate content of sugar-beet leaves, and on translocation. *Ann. Appl. Biol.* **38**, 276–288 (1951).
53. Chen, J. et al. Beneficial effects of Biochar-Based organic fertilizers on nitrogen assimilation, photosynthesis, and sucrose synthesis of sugar beet (*Beta vulgaris* L.). *Int. J. Plant. Prod.* **16**, 755–768 (2022).
54. Hoffmann, C. M. & Kluge-Severin, S. Growth analysis of autumn and spring sown sugar beet. *Eur. J. Agron.* **34**, 1–9 (2011).

55. PN-ISO 11265:1997 Soil quality—determination of the specific electrical conductivity (1997).
56. ISO 11466:1995—Soil quality—extraction of trace elements soluble in aqua regia (1995).
57. Pogrzeba, M., Rusinowski, S. & Krzyżak, J. Macroelements and heavy metals content in energy crops cultivated on contaminated soil under different fertilization—case studies on autumn harvest. *Environ. Sci. Pollut. Res.* **25**, 12096–12106 (2018).
58. ISO 13878:1998. Determination of Total Nitrogen Content by Dry Combustion (“Elemental Analysis”) (1998).
59. Egnér, H., Riehm, H. & Domingo, W. R. Investigations on chemical soil analysis as the basis for estimating the nutrient status of soils. II. Chemical methods of extraction for phosphorus and potassium determinations. *K. Lantbr. Ann.* **26**, 199–215 (1960).
60. Rossi, V. & Battilani, P. CERCOPRI: a forecasting model for primary infections of cercospora leaf spot of sugarbeet <sup>1</sup>. *EPPO Bull.* **21**, 527–531 (1991).
61. Sentinel-hub EO-Browser3. [https://apps.sentinel-hub.com/eo-browser/?zoom=10&lat=41.9&lng=12.5&themeId=DEFAULT-TH\\_EME&toTime=2024-08-29T10%3A26%3A39.017Z](https://apps.sentinel-hub.com/eo-browser/?zoom=10&lat=41.9&lng=12.5&themeId=DEFAULT-TH_EME&toTime=2024-08-29T10%3A26%3A39.017Z). Access 29.08.2024
62. Sinergise, S. H. by. LAI (Leaf Area Index). *Sentinel Hub custom scripts*. <https://custom-scripts.sentinel-hub.com/custom-scripts/sentinel-2/lai/>. Access 29.08.2024.
63. Strasser, R. J., Tsimilli-Michael, M. spsampsps Srivastava, A. Analysis of the Chlorophyll a Fluorescence Transient. In *Chlorophyll a Fluorescence* (eds. Papageorgiou, G. C. spsampsps Govindjee) vol. 19 321–362 (Springer, 2004).
64. Ran, X. et al. Assessment of growth rate, chlorophyll a fluorescence, lipid peroxidation and antioxidant enzyme activity in Aphanizomenon flos-aquae, *Pediastrum simplex* and *Synechococcus acus* exposed to cadmium. *Ecotoxicology* **24**, 468–477 (2015).
65. Schansker, G., Tóth, S. Z. & Strasser, R. J. Dark recovery of the Chl a fluorescence transient (OJIP) after light adaptation: the qT-component of non-photochemical quenching is related to an activated photosystem I acceptor side. *Biochimica Et Biophys. Acta (BBA) - Bioenergetics.* **1757**, 787–797 (2006).
66. Official Methods of Analysis, 22nd Edition. *AOAC International* (2023). <https://www.aoac.org/official-methods-of-analysis/>. Access 29.08.2024.

## Author contributions

A.B.: Conceptualization, Methodology, Supervision, Resources, Writing—Original draft preparation, Writing—Reviewing and Editing. S.R.: Methodology, Data curation, Visualization, Writing—Original draft preparation. J.K.: Data curation, Resources, Writing—Original draft preparation. A.K.S.: Writing—Reviewing and Editing. B.S.: Investigation, R.S.: Investigation, Writing—Reviewing and Editing. K.Sm.: Data curation, Visualization. E.M.: Writing—Reviewing and Editing. K.Si.: Conceptualization, Methodology, Validation, Resources, Investigation, Writing—Original draft preparation, Writing—Reviewing and Editing.

## Declarations

### Competing interests

The authors declare no competing interests.

### Additional information

**Supplementary Information** The online version contains supplementary material available at <https://doi.org/10.1038/s41598-025-03968-8>.

**Correspondence** and requests for materials should be addressed to K.S.

**Reprints and permissions information** is available at [www.nature.com/reprints](http://www.nature.com/reprints).

**Publisher's note** Springer Nature remains neutral with regard to jurisdictional claims in published maps and institutional affiliations.

**Open Access** This article is licensed under a Creative Commons Attribution-NonCommercial-NoDerivatives 4.0 International License, which permits any non-commercial use, sharing, distribution and reproduction in any medium or format, as long as you give appropriate credit to the original author(s) and the source, provide a link to the Creative Commons licence, and indicate if you modified the licensed material. You do not have permission under this licence to share adapted material derived from this article or parts of it. The images or other third party material in this article are included in the article's Creative Commons licence, unless indicated otherwise in a credit line to the material. If material is not included in the article's Creative Commons licence and your intended use is not permitted by statutory regulation or exceeds the permitted use, you will need to obtain permission directly from the copyright holder. To view a copy of this licence, visit <http://creativecommons.org/licenses/by-nc-nd/4.0/>.

© The Author(s) 2025